Batch sorption and spectroscopic speciation studies of neptunium uptake by montmorillonite and corundum

O. Elo [a,*], K. Müller [b], A. Ikeda-Ohno [b], F. Bok [b], A.C. Scheinost [b,c], P. Hölttä [a], N. Huittinen [b]

[a] *Laboratory of Radiochemistry, Department of Chemistry, P.O. Box 55, FIN-00014 University of Helsinki, Finland*
[b] *Helmholz-Zentrum Dresden-Rossendorf, Institute of Resource Ecology, P.O. Box 510119, D-01314 Dresden, Germany*
[c] *The Rossendorf Beamline, The European Synchrotron Radiation Facility (ESRF), P.O. Box 40220, F-38043 Grenoble, France*

Abstract

Detailed information on neptunium(V) speciation on montmorillonite and corundum surfaces was obtained by batch sorption and desorption studies combined with surface complexation modelling using the Diffuse Double-Layer (DDL) model, *in situ* time-resolved Attenuated Total Reflection Fourier-Transform Infrared (ATR FT-IR) and X-ray absorption (XAS) spectroscopies. The pH-dependent batch sorption studies and the spectroscopic investigations were conducted under carbonate-free conditions in 10 mM $NaClO_4$ or 10 mM NaCl. Solid concentrations of 0.5 g/l and 5 g/l were used depending on the experiment. The neptunium(V) desorption from the two mineral surfaces was investigated at pH values ranging from 8 to 10, using the replenishment technique. Neptunium(V) was found to desorb from the mineral surface, however, the extent of desorption was dependent on the solution pH. The desorption of neptunium(V) was confirmed in the ATR FT-IR spectroscopic studies at pH 10, where all of the identified inner-sphere complexed neptunium(V), characterized by a vibrational band at 790 cm^{-1}, was desorbed from both mineral surfaces upon flushing the mineral films with a blank electrolyte solution. In XAS investigations of neptunium(V) uptake by corundum, the obtained structural parameters confirm the formation of an inner-sphere complex adsorbed on the surface in a bidentate fashion. As the inner-sphere complexes found in the IR-studies are characterized by identical sorption bands on both corundum and montmorillonite, we tentatively assigned the neptunium(V) inner-sphere complex on montmorillonite to the same bidentate complex found on corundum in the XAS investigations. Finally, the obtained batch sorption and spectroscopic results were modelled with surface complexation modelling to explain the neptunium(V) speciation on montmorillonite over the entire investigated pH range. The modelling results show that cation exchange in the interlayer space as well as two pH-dependent surface complexes are required to fully explain the neptunium(V) speciation on the montmorillonite surface.

© 2016 The Author(s). Published by Elsevier Ltd. This is an open access article under the CC BY-NC-ND license (http://creativecommons.org/licenses/by-nc-nd/4.0/).

Keywords: Neptunium(V); Sorption; Montmorillonite; Corundum; Surface complexation; X-ray absorption spectroscopy; ATR FT-IR spectroscopy

1. INTRODUCTION

The neptunium (Np) isotope Np-237 is an actinide of concern in safety assessments of spent nuclear fuel (SNF) repositories. This radiotoxic isotope has an extremely long half-life ($t_{1/2} = 2.144 \times 10^6$ y) making it a major dose contributor to the radiation inventory in nuclear waste after one hundred thousand years (Hursthouse et al., 1991; Kaszuba and Runde, 1999; Zhao et al., 2014). In mildly oxic conditions Np is stable in the pentavalent oxidation state as the neptunium(V) cation (NpO_2^+), which is rather

---

soluble, poorly retained by solid phases and, thus, susceptible to migration by groundwater in the far field of a SNF repository (Viswanathan et al., 1998; Kaszuba and Runde, 1999; Kozai et al., 2014). In order to quantitatively describe the mobility of neptunium(V) in the environment, a thorough understanding of the sorption behaviour of the cation on artificial and natural barrier materials is required. Surface retention in general is especially effective on clay minerals possessing large surface areas and strong retention capacities. For this reason clay minerals are envisioned as both potential host rock materials and as buffers and fillers in various repository designs. One of the important minerals in this context is montmorillonite, the main constituent in bentonite clay which is being considered as a buffer material in several repository concepts under consideration in e.g. Scandinavia, France and Switzerland. Montmorillonite is known to readily retain radionuclides either through cation exchange in the interlayer space (Birgersson and Karnland, 2009; Hartmann et al., 2011) or by surface complexation onto reactive sorption sites prevalently on the edge sites (Bradbury and Baeyens, 2002; Sabodina et al., 2006; Zavarin et al., 2012). A number of studies investigating radionuclide sorption onto montmorillonite can be found (Marques Fernandes et al., 2012; Missana et al., 2014; Soltermann et al., 2014). However, only few of them deal with the uptake of neptunium(V) (Turner et al., 1998; Nagasaki and Tanaka, 2000; Bradbury and Baeyens, 2006; Sabodina et al., 2006; Zavarin et al., 2012; Kozai et al., 2014). In addition, none of these studies involve detailed spectroscopic investigations that would explain the speciation of neptunium(V) on the montmorillonite surface, which could eventually describe the sorption mechanism of this mineral. In the present study we have investigated neptunium(V) sorption and speciation on a natural montmorillonite mineral under simplified but, when possible, under environmentally relevant conditions. Natural minerals often have multiple functional surface groups, which makes the surface speciation more complex. In this context, this study has employed the aluminium oxide corundum (α-Al_2O_3) as a model phase for reactive aluminol groups on the montmorillonite mineral surface. We have conducted batch sorption and desorption experiments to quantify the uptake of neptunium(V) by the minerals and the extent of desorption from the mineral surfaces, respectively. The neptunium(V) batch sorption data on montmorillonite has been modelled with the Diffuse Double-Layer model to extract complexation constant for the formed neptunium(V) surface species. Detailed information on the coordination environment of neptunium(V) on the mineral surfaces was obtained by Attenuated Total Reflection Fourier-Transform Infrared (ATR FT-IR) and X-ray absorption spectroscopies (XAS).

2. MATERIALS AND METHODS

2.1. Mineral characterization

The homoionic sodium montmorillonite used in this study has been isolated from Wyoming Volclay MX-80 bentonite and purified by B⁺Tech Oy, Finland. The XRD diffractogram obtained for montmorillonite showed impurities from quartz and paragonite (Fig. 1, left). These impurities may have been transferred during the purification from the MX-80 bentonite powder (Kumpulainen and Kiviranta, 2010). The surface ζ-potential of 0.25 g/l montmorillonite measured under carbonate-free conditions in 10 mM NaCl by microelectrophoresis (Zeta Sizer Nano, Malvern Instruments) showed a constant negative charge over the entire investigated pH-range, Fig. 1 (right). Thus, no isoelectric point (IEP) corresponding to a net surface charge of zero could be assigned for the mineral. The specific surface area of montmorillonite was found to be 49.8 m^2/g with the N_2-BET technique. The mineral was used as received in the batch sorption and spectroscopic investigations.

Corundum (α-Al_2O_3) was provided by Taimei Chemicals, Tokyo, Japan (TAIMICRON TM-DAR). The powder has been thoroughly characterized in Kupcik et al. (2016) and found to have a crystalline purity of >99.99% in XRD and XPS investigations. Thus, the corundum powder was used without further purification in all studies. Results from the mineral characterizations are compiled in Table 1.

2.2. Batch adsorption and desorption investigations

2.2.1. Neptunium(V) adsorption investigations

All batch sorption experiments were conducted in a N_2-glove box to exclude the formation of soluble neptunium(V)-carbonato complexes that influence the uptake and speciation of neptunium(V) on the solid surfaces. 10 mM $NaClO_4$ was always used as background electrolyte and the montmorillonite or corundum concentration was kept constant at either 0.5 g/l (similar to the solid concentration in the ATR FT-IR experiments) or 5 g/l (as used for the XAS experiments). Batch sorption experiments as a function of pH (pH-edges) were conducted in 20 ml polypropylene vials using a constant neptunium concentration of 10^{-6} M across the pH range 4–11. pH adjustments were done with 0.01–1 M NaOH and $HClO_4$ solutions. All samples were allowed to equilibrate in the glove box under constant shaking for 7 or 30 days before phase separation at minimum 3830 g (6000 rpm) for 60 min. The amount of adsorbed neptunium(V) was analysed from the supernatant with liquid scintillation counting (Tri-Carb 3100 TR) using α/β-discrimination to separate out the β disintegrations from the Np-237 daughter nuclide Pa-233. To rule out a possible carbonate contamination originating from the mineral itself, we performed leaching tests on 0.5 g/l and 5 g/l montmorillonite suspensions over 7 and 30 days at pH-values of 9, 10 and 11. After equilibration, the carbonate content was measured with a carbon dioxide electrode (Carbon Dioxide Ion Selective Electrode, Thermo Scientific) with a detection limit of 10^{-4} M.

2.2.2. Neptunium(V) desorption investigations

Desorption experiments were conducted to investigate the extent of desorption from the montmorillonite and corundum surfaces. The experimental conditions were kept similar to the batch adsorption investigations as explained above, i.e. N_2-atmosphere, montmorillonite or corundum
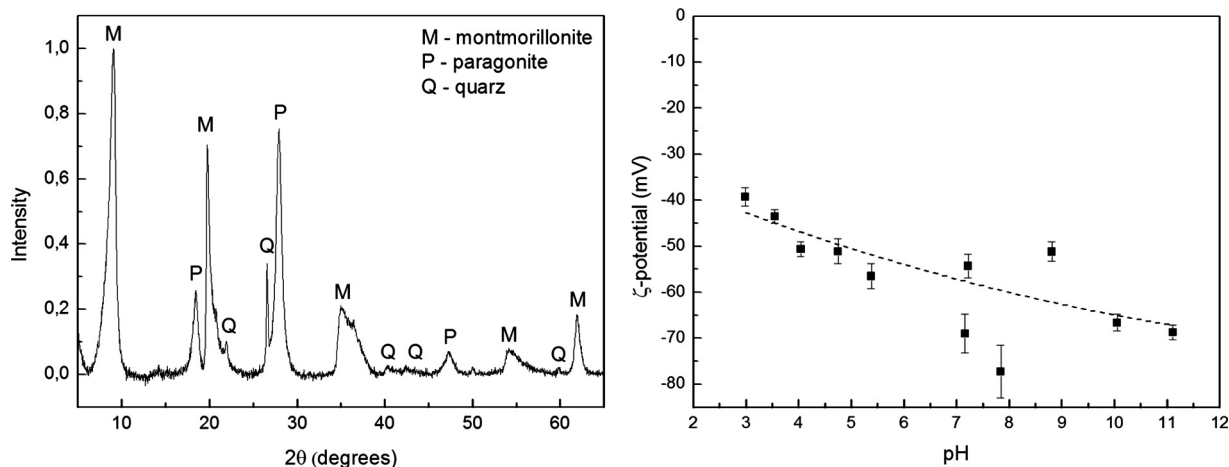
Fig. 1. Left: XRD pattern of the purified montmorillonite (B$^+$Tech). Right: ζ-potential of 0.25 g/l montmorillonite as a function of pH measured under carbonate-free conditions in 10 mM NaCl.

Table 1
Characterization data on montmorillonite and corundum.

	Montmorillonite	Corundum
BET [m²/g]	49.8[*]	14.5[**]
Grain size [μm]	–	150–200[**]
IEP (NaCl)	Constant negative charge[*]	8.8[**]

[*] This study.
[**] Kupcik et al. (2016).

concentration 5 g/l, neptunium(V) concentration 10^{-6} M and 10 mM NaClO$_4$. In the acidification desorption experiment, that was conducted only for montmorillonite, the pH of the mineral suspension was brought to ~8 and neptunium(V) was allowed to adsorb on the montmorillonite surface. After an equilibration time of 7 days the suspension was acidified to a pH value of approximately 5, and the neptunium(V) desorption was monitored as a function of time by taking small aliquots of the suspension 1 h to 15 days after acidification. The goal behind this experiment was to investigate whether the kinetics of adsorption and desorption are the same. The second desorption experiment, conducted using the replenishment technique, was designed to simulate the flushing procedure at constant pH in the *in situ* ATR FT-IR investigations explained later in the text, through exchanging the TRIS (tris-hydroxyme thyl-aminomethane) buffered (pH 8), CHES (2-(cyclohexyla mino)ethanesulfonic acid) buffered (pH 9 or 10) background electrolyte (10 mM NaClO$_4$) of the montmorillonite suspension every 2–3 days or 7 days. A constant pH was required for the replenishment desorption experiments to avoid pH fluctuations that could contribute to the desorption of neptunium(V), as the influence of flushing on the desorption process was the main focus. The phase separation in the desorption experiments was done by centrifugation at minimum 3830 *g* (6000 rpm) for 60 min. A small (1 ml) aliquot of the separated supernatant was taken for liquid scintillation counting to determine the desorbed amount of neptunium(V) in the experiments.

2.3. Neptunium(V) speciation investigations

2.3.1. ATR FT-IR spectroscopy

For the molecular identification of neptunium(V) surface species on corundum and montmorillonite Attenuated Total Reflection Fourier-Transform Infrared (ATR FT-IR) spectroscopy was applied. The method provides *in situ* information on the neptunium(V) sorption complexes based on the characteristic vibrational modes of the neptunium(V) cation. Infrared spectra were measured from 1800 to 600 cm^{-1} on a Bruker Vertex 70/v vacuum spectrometer, equipped with a Mercury Cadmium Telluride (MCT) detector. The spectral resolution was 4 cm^{-1} and spectra were averaged over 256 scans. A horizontal diamond crystal with nine internal reflections (DURA SamplIR II, Smiths Inc.) was used. Further details on the experimental ATR FT-IR setup are compiled in Müller et al. (2012).

In situ vibrational spectroscopic experiments are based on the principle of reaction-induced difference spectroscopy, in which spectral changes related to selectively induced changes of the investigated sample are detected. IR single beam spectra of a mineral film, prepared as a stationary phase, are continuously recorded while it is flushed by a mobile phase, comprising aqueous solutions for equilibration and for induced sorption. The progress of the sorption process is monitored with a time resolution in the sub-minute time range, since the acquisition time of each single beam spectrum is about 30 s. The very small adsorption changes (optical density $\geqslant 10^{-5}$) in the spectra caused by addition of neptunium(V) on the mineral film, can be depicted as difference spectra calculated from the single beam spectra recorded before and after neptunium (V) introduction.

The mineral film on the surface of the ATR diamond crystal was prepared by pipetting aliquots of corundum or montmorillonite suspensions on the crystal followed by drying with a gentle stream of N$_2$. This procedure was repeated until an average mass density of 0.2 mg/cm^2 was obtained on the crystal. The mineral film was conditioned by flushing with the blank solution (0.01 M NaCl, pH 10)

for 60 min using a flow cell ($V = 200$ µl) at the rate of 100 µl/min. Subsequently, the sorption reaction was induced by rinsing the stationary phase with the neptunium(V) solution (50 µM in 0.01 M NaCl at pH 10) for 120 min. Finally, the loaded mineral phase was flushed again with the blank solution (60 min) in order to gain more information on the desorption extent of the sorbed neptunium(V) species. All reagents were prepared in D_2O to avoid spectral overlap caused by O–H vibrations in the infrared region of interest. NaCl was used as a background electrolyte instead of ClO_4^- as the Na^+ and Cl^- ions show no adsorption in the investigated frequency range.

2.3.2. X-ray absorption spectroscopy

X-ray absorption spectra, including both X-ray absorption near-edge structure (XANES) and extended X-ray absorption fine structure (EXAFS) regions, were collected at Np L_{III}-edge on the Rossendorf Beamline (ROBL) (Matz et al., 1999) at the European Synchrotron Radiation Facility (ESRF) under dedicated ring operating conditions of 6 GeV and 150–200 mA. A Si(111) double-crystal monochromator was employed to monochromatize the incoming synchrotron X-rays. A flat, meridionally-bent, 140-cm long Rh-coated silicon mirror was used to collimate the beam into the monochromator. The monochromatic beam was further conditioned by using a toroidal, 120-cm long Rh-coated silicon mirror. Both mirrors provide a suppression of higher harmonics by at least four orders of magnitude. The spectra were collected at 15 K in fluorescence mode with gas-filled ionization chambers (I_0 and I_{ref}) and a 13-element Ge solid state detector (I_F, Canberra). Energy calibration of the collected spectra was performed by the simultaneous measurement of reference Y foil (Y K-edge defined as 17038 eV at the first XANES inflection point). At least four spectra were collected for each sample and the obtained spectra were averaged for further data analysis. The acquired spectra were analysed according to a standard procedure (Koningsberger and Prins, 1988) on the programme WinXAS (version 3.2) (Ressler, 1998). EXAFS theoretical fitting was performed both in k-space (i.e. EXAFS oscillation spectra) and R-space (i.e. Fourier transforms: FTs). EXAFS theoretical phase and amplitude required for the theoretical fitting were calculated by the programme code FEFF 8.20 (Ankudinov et al., 1998) based on the hypothetical cluster "hydrated $Np^VO_2^+$ sorbed on gibbsite" employed in the study by Gückel et al. (2013) and Virtanen et al. (2016). The threshold energy, $E_{k=0}$, was defined as the first XANES inflection point of each spectrum. The amplitude reduction factor, S_0^2, was fixed at 0.9, while the shifts in $E_{k=0}$ were varied but constrained to be the same value for all the shells.

XAS measurements were performed for the neptunium(V)-corundum samples only, due to a zirconium impurity in the natural montmorillonite mineral interfering with the Np EXAFS region. Thus, our XAS data is limited to investigations on the interaction of neptunium(V) with surface aluminol groups. On the montmorillonite surface, two functional groups, silanol and aluminol, are known to participate in metal adsorption. However, in the alkaline pH region aluminol groups are dominating the metal ion sorption (Turner et al., 1996; Wang et al., 2001; Del Nero et al., 2004), thus, speaking for the use of corundum as model phase for the surface functional groups on the clay mineral surface. Furthermore, several studies have indicated that oxide minerals serve as a good model phase for clays (Stumpf et al., 2001; Huittinen et al., 2009; Müller et al., 2009). The XAS samples were prepared using a constant neptunium(V) and corundum concentration of 20 µM and 5 g/l, respectively in 10 mM NaCl. The sample pH was adjusted to either pH 9 or 10, where sufficient neptunium(V) sorption on the mineral surfaces was found to occur (Fig. 2). After an equilibration time of one week the samples were centrifuged (3830 g, 6000 rpm/60 min) and the supernatant was separated from the solid phase. The remaining wet paste was transferred into Teflon sample holders that where further sealed by melting the Teflon lid. The sample preparation was performed in an inert glove box to avoid exposure of the wet paste sample to atmospheric carbon dioxide. Once the samples were removed from the box, they were immediately immersed and stored in liquid nitrogen until XAS measurements.

2.4. Surface complexation modelling of batch sorption data

In order to promote application of surface complexation modelling data records in the modelling of more complex (natural and anthropogenic) scenarios, the rather simple Diffuse Double-Layer (DDL) model was selected, which is already implemented in various geochemical codes (e.g. PHREEQC, Geochemist's Workbench). In addition, the Diffuse Double-Layer model can be better extended to other chemical conditions like natural pore waters than more sophisticated models (e.g. CD-MuSiC) that are bound to specific background electrolytes and specific surface planes used in the parametrization. Previously, the DDL model has been successfully used to model neptunium(V) sorption on corundum, Virtanen et al. (2016). For this reason the same model was applied in our study. However, the DDL model has some drawbacks when it comes to modelling metal ion sorption on clay minerals as shown in e.g. Bradbury and Baeyens (1997). Surface complexation modelling (SCM) was applied to the experimental neptunium(V) batch sorption data on montmorillonite. All fits were run with a consistent set of parameters for the surface site density (SSD = 6.24×10^{-5} mol/g mineral), surface protolysis constants ($\log K_{a1} = 6.05$, $\log K_{a2} = -7.79$), derived from discontinuous back titration data with FITEQL (Tachi et al., 2010) and specific surface area ($A_s = 49.8$ m^2/g) (this study). The calculated IEP from these protolysis constants was approximately 6.92, which was well in accordance with the experimentally determined pH$_{PZC}$ value of 6.5 reported for the montmorillonite edge surfaces in Tombácz and Szekeres (2004). Thermodynamic data for the modelling was taken from the NEA TDB including its update (Lemire et al., 2001; Guillaumont et al., 2003). Despite the drawbacks of the DDL model when it comes to clay minerals, the model was implemented in the present study to explain the sorption of neptunium(V) on montmorillonite. To test the robustness of our DDL model we applied the model to another available
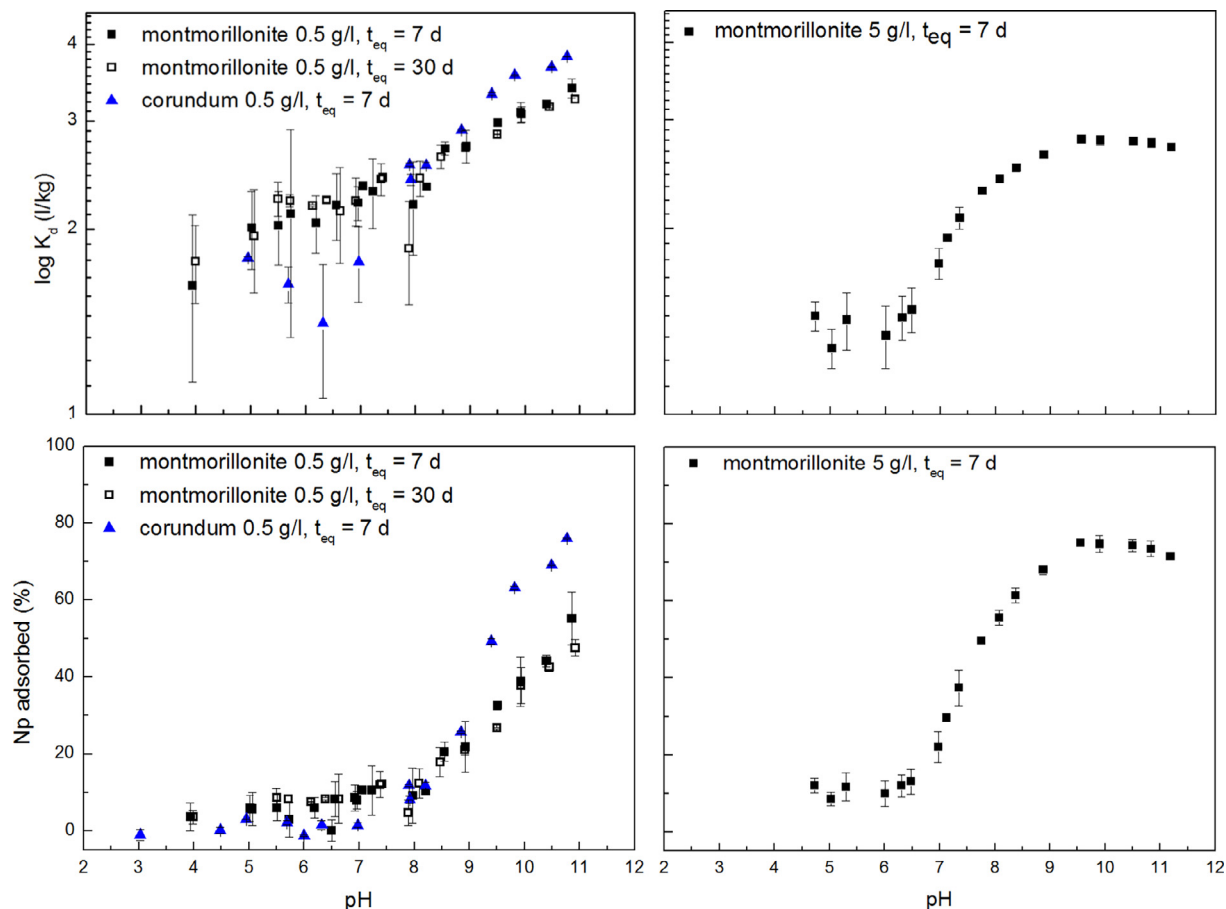
Fig. 2. Sorption of 10^{-6} M neptunium(V) onto 0.5 g/l montmorillonite and corundum (left) and 5 g/l montmorillonite (right) as a function of pH after 7 and 30 days equilibration time in 10 mM $NaClO_4$. The sorption data is given both as $\log K_d$ vs. pH (above) and as the sorption percentage vs. pH (below).

set of neptunium(V) sorption data on montmorillonite (SI Fig. S1). The DDL model was applied using PHREEQC (version 3.1.5-9113) (Parkhurst and Appelo, 2013) coupled with the software UCODE2005 (Poeter et al., 2006).

3. RESULTS

3.1. Batch adsorption and desorption investigations

3.1.1. Neptunium(V) adsorption investigations

The pH-dependent batch sorption data for neptunium (V) uptake on 0.5 g/l corundum and montmorillonite after 7 and 30 days equilibration times are shown in Fig. 2 (left).

The neptunium(V) uptake increased at pH >7 for both minerals but the overall sorption percentage remained rather low over the entire investigated pH range. No increase in the neptunium(V) uptake was detected as the equilibration time was increased to 30 days, indicating that the sorption reaction has reached a quasi-equilibrium state already after 7 days. For montmorillonite a constant neptunium(V) uptake of 5.1 ± 2.6% ($\log K_d = 2.0 \pm 0.2$ l/kg) and 12.8 ± 4.0% ($\log K_d = 1.5 \pm 0.1$ l/kg) for 0.5 g/l and 5 g/l, respectively, was seen in the circumneutral to acidic pH range in contrast to corundum where no neptunium(V)

uptake occurred below pH 7. This neptunium(V) uptake could speak for cation exchange on the negatively charged planar sites on the montmorillonite surface as found for neptunium(V) sorption on montmorillonite by Turner et al. (1998), Bradbury and Baeyens (2006), Zavarin et al. (2012) and Benedicto et al. (2014). Such ion exchange is unlikely to occur on the corundum surface due to the high isoelectric point of pH_{IEP} 8.8 and the absence of structural substitution reactions causing a permanent negative surface charge. As the solid concentration was increased from 0.5 g/l to 5 g/l, a shift of the pH edge toward lower pH values and a higher maximum neptunium(V) uptake of 80% was observed, Fig. 2 (right). In addition, a slight decrease of the neptunium(V) uptake above pH 10 was seen for this mineral concentration that is not witnessed in the 0.5 g/l suspension.

3.1.2. Neptunium(V) desorption investigations

Results from the desorption studies using the replenishment technique are presented in Fig. 3 (left and middle). Desorption of neptunium(V) from the corundum and montmorillonite surfaces decreased with increasing pH, speaking for the formation of a surface complex that is more strongly bound to the surface than at lower pH values
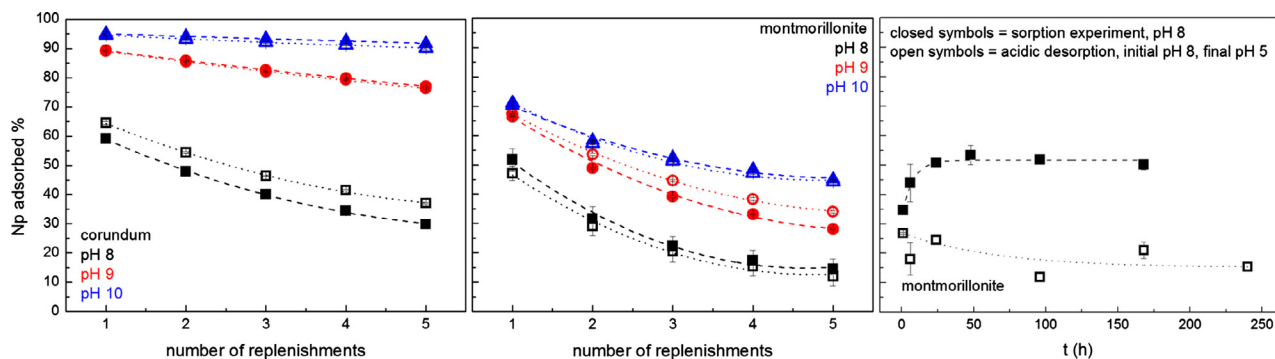
Fig. 3. Neptunium(V) desorption by changing the background electrolyte to a fresh one either every 2–3 days (open symbols) or once a week (closed symbols) for corundum (left) and montmorillonite (middle). A kinetic experiment of neptunium(V) sorption (closed symbols) onto montmorillonite and desorption from the surface after acidification of the mineral suspension (open symbols) is presented on the right. The extent of desorption of neptunium(V) is also presented as log K_d in SI Fig. S2.

(Fig. 3). The neptunium(V) desorption behaviour from corundum was independent of the exchange interval for all of the investigated pH values (Fig. 3, left) and the desorption extent in general was lower than for montmorillonite. At pH 10, practically no neptunium(V) desorption from the corundum surface was seen anymore. At pH 8, 75% of neptunium(V) was desorbed from the montmorillonite surface after five electrolyte changes independent of the exchange interval, i.e. exchange every 2–3 days, Fig. 3 (middle, open squares) or 7 days, Fig. 3 (middle, solid squares). At this pH and at pH 10, the exchange interval was not seen to influence the extent of desorption of neptunium(V). The situation was slightly different at pH 9, where the shorter exchange interval of 2–3 days showed a slightly lower extent of desorption of 50% than the longer exchange interval of 7 days where 55% of the sorbed actinide was desorbed. Acidic desorption experiments conducted for montmorillonite (Fig. 3, right) also showed that neptunium(V) was desorbed from the mineral surface, at least to a certain extent. Here, the neptunium(V) ion exchange fraction was not removed under the acidic pH conditions (pH = 5) but a desorption plateau at approximately 15% neptunium(V) uptake was obtained approximately 50 h after acidification.

3.2. Speciation investigations

3.2.1. ATR FT-IR spectroscopy

Time-resolved infrared spectra of neptunium(V) sorption on corundum (A) and montmorillonite (B) are presented in Fig. 4.

The in situ sorption experiments of this study were described by three stages. In the first step, the mineral film was conditioned to an appropriate pH and ionic strength for 60 min. The difference spectrum, referred to as "conditioning", was calculated from a single beam spectra recorded during 50–60 min rinsing the mineral film with blank solution. This spectrum reflects the stability of the film under the chosen conditions and serves as a measure of quality for the experimental setup. In the second step, the neptunium(V) sorption process onto the mineral film was performed for the next 120 min. Difference spectra, referred to as "sorption", were calculated from the last sin-
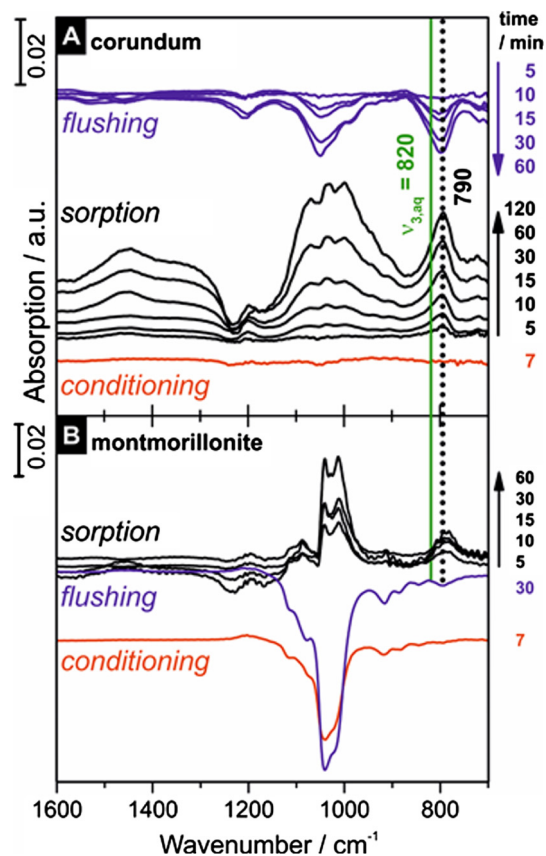

Fig. 4. In situ time-resolved ATR FT-IR spectra of neptunium(V) sorption on corundum (A) and montmorillonite (B) at pH 10 (50 μM neptunium(V), D_2O, 0.01 M NaCl, N_2, ~0.2 mg mineral cm^{-2}). The spectra of the conditioning (red traces), sorption (black traces) and flushing (blue traces) processes are shown at different time intervals. Indicated values are in cm^{-1}.

gle beam spectra obtained at the conditioning stage, and from spectra obtained at different time intervals after starting the induced sorption process. In the last step, the mineral film was again flushed with the blank solution for further 60 min ("flushing"). The respective difference

spectra calculated from single beam spectra recorded at the end of the sorption stage of the experiment provides additional information on the desorption extent of the sorption process and weakly bound metal species were predominantly identified.

For corundum (Fig. 4A) a constant baseline of the conditioning spectrum (red trace) was obtained, indicating that the corundum film was sufficiently stable for the *in situ* spectroscopic sorption experiments. For montmorillonite (Fig. 4B), the conditioning spectrum showed a strong negative peak at ~1100 cm^{-1} which can be attributed to vibrations of the silanol surface functionalities. The negative sign of this peak indicated a constantly slow removal of montmorillonite particles from the ATR crystal surface upon flushing. However, the total amount of removed montmorillonite during the whole sorption experiment was very low, because transmission spectra of the dried film obtained just subsequent to film preparation and after the flow-through experiment indicated a difference of maximum 5%.

In time-resolved spectra of the sorption stage several positive peaks were detected (black traces) on both minerals. The spectral region above 1000 cm^{-1} was characterized by strong overlapping bands from vibrational modes of the solid phase. These bands represented alterations at the mineral–water interface related to the reactions with the neptunium(V) cation. As these bands are generally less specific and cannot be accurately assigned to distinct molecular functional groups, a detailed interpretation is not given here. However, similar bonds have also been observed for neptunium(V) sorption on Al(OH)$_3$ (Gückel et al., 2013), Fe$_2$O$_3$ (Müller et al., 2015), TiO$_2$ and SiO$_2$ (Müller et al., 2009). The progress of neptunium(V) accumulation on the mineral surfaces could be monitored from the time-dependent increase of the adsorption band at 790 cm^{-1}.

This peak was assigned to the antisymmetric stretching mode ν_3 of adsorbed neptunium(V). The presence of one single band showing a constant frequency maximum and band width thorough the sorption time of 120 min for corundum (Fig. 4A) and 60 min for montmorillonite (Fig. 4B) indicated the presence of only one type of surface species. After about 60 min, the intensity increase on corundum stagnated indicating that a steady-state at the interface was reached. On montmorillonite a saturation of available surface sites by adsorbed neptunium(V) was seen already after 15 min. Subsequent to sorption, "flushing" of the mineral film with blank solution was performed in order to provide information on surface species which can be easily removed. The difference spectra in Fig. 4 (blue traces) were calculated from the spectra recorded at the end of the sorption step and after different time steps of flushing. In contrast to the sorption data, negative peaks showing significantly reduced intensities are observed between 1200 and 900 cm^{-1} and at 790 cm^{-1}. The latter band can be attributed to neptunium(V) which was released from the mineral film. In contrast to the batch desorption experiments at this pH where the desorption of neptunium(V) from the corundum surface was very low, the flushing procedure seemed to remove almost all of the initially bound complex.

3.2.2. X-ray absorption spectroscopy

The Np L$_{III}$-edge XANES spectra of the neptunium(V) absorbed on corundum (SI Fig. S3) showed a characteristic shoulder structure at around 17.63 keV, which originated from the trans-dioxo arrangement of neptunium(V) (i.e., neptunyl(V)) in the samples (Soderholm et al., 1999). This confirmed the dominant presence of neptunium(V) in the samples. The EXAFS spectra for corundum samples at
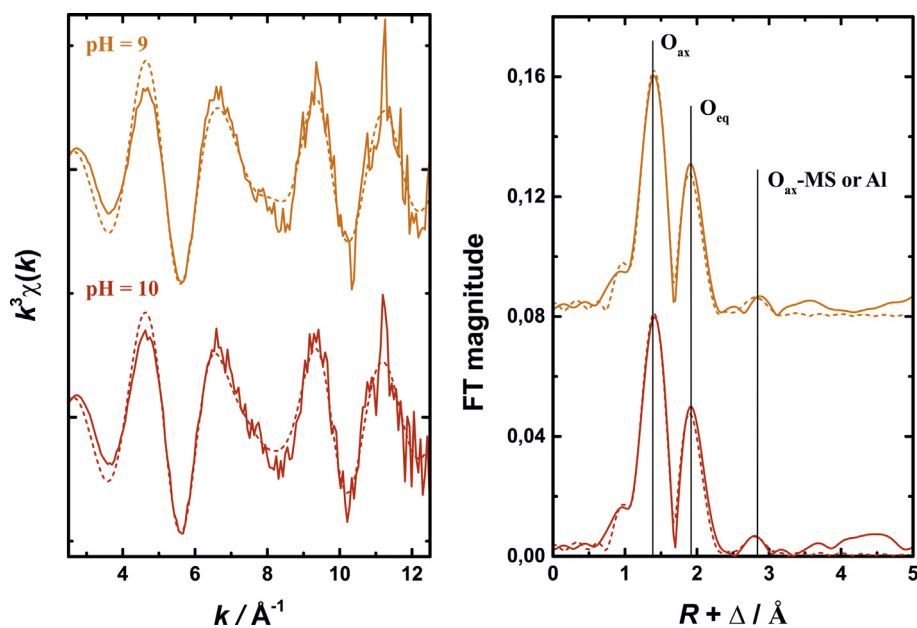

Fig. 5. k^3-weighted Np L$_{III}$-edge EXAFS spectra for neptunium(V) adsorbed on corundum at pH 9 and 10 (left) and their corresponding Fourier transforms (right). Solid lines; experimental data, dotted lines; theoretical fitting. Phase shifts (Δ) are not corrected in the FTs.

pH 9 and 10 and their corresponding Fourier transforms (FTs) are presented in Fig. 5. The EXAFS structural parameters obtained from theoretical curve fitting are summarized in Table 2.

The highest FT peak appeared at around $R + \Delta = 1.4$ Å and corresponded to the two axial oxygens (O_{ax}) of the neptunium(V) cation, while the second highest peak at around $R + \Delta = 2.0$ Å reflected the ligand coordination in the equatorial plane of the neptunium(V) cation (Ikeda-Ohno et al., 2008). The present neptunium(V) samples only contain H_2O, NaCl, and corundum in addition to the actinide cation. The existence of neptunium(V) hydroxide complexes at pH 10 is highly unlikely due to the speciation of neptunium(V) under the experimental conditions (Müller et al., 2015). In addition, the neptunium(V) hydroxide species was not detected in the ATR FT-IR spectra (Fig. 4). Since the coordination of Cl^- to neptunium(V) is expected to be negligible under the studied conditions, (Allen et al., 1997) the possible ligands coordinating to neptunium(V) cations are water molecules and functional sites on the corundum surface (i.e. aluminol groups), both of which interact with neptunium(V) *via* oxygens. Hence, it was reasonable to fit the second FT peak assuming the oxygen coordination shell (O_{eq}). The Np–O_{ax} and Np–O_{eq} interatomic distances obtained from EXAFS theoretical fitting were 1.86 Å and 2.45–2.46 Å, respectively, which were in agreement with those obtained from the neptunium(V) species absorbed on gibbsite (Gückel et al., 2013). The FTs in Fig. 5 showed an additional peak at around $R + \Delta = 2.84$ Å, which could be attributed to either single scattering of Al on the corundum surface (Fig. 5) or multiple scattering (MS) paths associated with the linear O_{ax}–Np–O_{ax} arrangement of neptunium(V) cations (Ikeda-Ohno et al., 2008). It is possible that the neptunium(V) attachment on the corundum surface caused a slight distortion of the linear O_{ax}–Np–O_{ax} arrangement of neptunium(V) cations, which would significantly lower the scattering amplitude of the MS paths. Thus, in analogy with the studies by Gückel et al. (2013) and Arai et al. (2007) investigating neptunium(V) sorption on gibbsite and hematite, respectively, we assigned the third FT peak at around $R + \Delta = 2.8$ Å to a mineral constituent atom. The peak could be very well fitted using an edge-sharing neptunium(V) species sorbed on the corundum surface in a bidentate fashion as illustrated in Fig. 6, resulting in a Np–Al distance of 3.33–3.38 Å.

3.3. Surface complexation modelling

To create a model based on a chemically realistic speciation for the neptunium(V) concentration used, a stepwise fitting of the experimental batch sorption data presented in Fig. 2 was done to extract surface complexation constants for the involved species.

In a first step the acidic pH region (pH < 7.2) showing a constant uptake of neptunium(V) on montmorillonite (see Fig. 2) was fitted using the ion exchange reaction shown in Eq. (1) following the Gaines-Thomas convention as implemented in PHREEQC (Appelo and Parkhurst,

2013). Data, with slight modifications, for the ion exchange reaction and the corresponding equations for Na^+ and H^+ were taken from Tachi et al. (2010).

$$\equiv X^- + NpO_2^+ \leftrightarrow \equiv XNpO_2 \qquad (1)$$
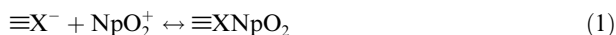
In a second step the pH edges of neptunium(V) adsorbed on 0.5 g/l and 5 g/l montmorillonite in 10 mM $NaClO_4$ were fitted using a bidentate surface complex that deprotonates both surface groups. Here, the fitting was conducted using the surface complexation reaction presented in Eq. (2), with $n = 0–3$ as well as binary combinations thereof. Although the spectroscopic results (see discussion in Section 4.1) did not give hints of a monodentate surface complex, the $\equiv XO–NpO_2$ complex was tested too, however, the results from the fitting did not support the further use of this complex in the modelling.

$$2\equiv XOH + NpO_2^+ + 3H_2O \leftrightarrow (\equiv XO)_2 NpO_2(OH)_n$$
$$(H_2O)_{(3-n)}^{(n+1)-} + (2+n)H^+ \qquad (2)$$
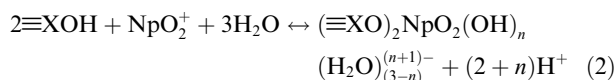
In addition to the ion exchange fraction, two pH-dependent species were required to explain our batch sorption data.

The best fit was obtained for a combination of a complex with $n = 0$ (species 1), that dominates the speciation above pH 9 and another surface complex given by Eq. (3) (species 2), where no deprotonation of the surface groups occurs, Fig. 7. Species 2 is not supported by any spectroscopic evidence, however, it was found to be necessary to include in order to describe the sorption behaviour of neptunium(V) onto montmorillonite (see SI Fig. S4 and Table S1).

$$2\equiv XOH + NpO_2^+ + 5H_2O \leftrightarrow (\equiv XOH)_2 NpO_2(H_2O)_5^+ \qquad (3)$$
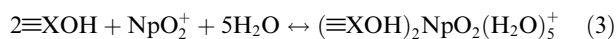
The water molecules in Eqs. (2) and (3) were not necessary for the surface complexation model. However, they have been added to the equations to reflect the correct chemistry of neptunium(V) in aqueous solution. All parameters and equations used for the modelling are compiled in Table 3, together with the obtained $\log K$ values for the neptunium(V) surface complexes.

4. DISCUSSION

4.1. Macroscopic and spectroscopic neptunium(V) sorption investigations

Our batch adsorption experiments of neptunium(V) uptake by montmorillonite showed two different regions of neptunium(V) attachment on the mineral surface: a small but constant uptake fraction of approximately 10% below pH 7 and a rapidly increasing, pH-dependent fraction above this pH (Fig. 2). The constant uptake of neptunium(V) on montmorillonite in the acidic pH range, could speak for sorption of the actinide on negatively charged planar sites through ion exchange. A slight decrease in neptunium(V) sorption on montmorillonite 5 g/l was observed at alkaline pH range (Fig. 2, right). A similar decrease in the neptunium(V) adsorption has been found in

Table 2
EXAFS structural parameters for Np L_{III}-edge EXAFS spectra given in Fig. 5.

Sample	$E_{k=0}$/keV	Scattering shell									S_0^2 (fixed)
		O_{ax}-SS[a]			O_{eq}-SS[a]			Al-SS[a]			$\Delta E_{k=0}$/eV[e]	
		CN[b]	R/Å[c]	σ^2/Å²[d]	CN[b]	R/Å[c]	σ^2/Å²[d]	CN[b]	R/Å[c]	σ^2/Å²[d]		
Np(V) on corundum, pH = 9	17.625	2.0	1.86	0.0020	4.7	2.45	0.0081	1.0	3.38	0.0082	0.89	0.9
Np(V) on corundum, pH = 10	17.625	2.0	1.86	0.0021	4.7	2.46	0.0081	1.1	3.33	0.0091	0.90	0.9

[a] SS; single scattering shells.
[b] Coordination number; Error ± <30%.
[c] Interatomic distance; Error ± <0.02 Å.
[d] Debye–Waller factors; Error ± <0.0010 Å².
[e] shift in threshold energy; Error ± <0.5 eV.

investigations on neptunium(V) sorption onto montmorillonite under atmospheric conditions (Turner et al., 1998; Tachi et al., 2010) where results showed that soluble neptunium(V)-carbonato complexes were formed above pH 8 that competed with the sorption reaction and subsequently decreased the uptake of neptunium(V) on the montmorillonite surface. However, our batch sorption and spectroscopic investigations were conducted under N_2-atmosphere to exclude the influence of atmospheric carbon dioxide on the neptunium(V) speciation. Furthermore, a carbonate contamination of our solutions used in the batch sorption experiments should cause a decrease of neptunium(V) sorption for both uptake curves (0.5 g/l and 5 g/l montmorillonite). Thus, a contamination of our reagents with CO_3^{2-} could be precluded. No carbonates leaching out from the mineral itself were detected by our carbonate sensitive electrode in any of our montmorillonite suspensions and a CO_3^{2-} concentration below 10^{-4} M (detection limit of the electrode) was not sufficient to explain the observed decrease in the neptunium(V) uptake above pH 9. Beside the presence of neptunium(V) and the electrolyte ions Na^+ and Cl^- or ClO_4^- in our batch sorption experiments the only other dissolved species present in our mineral suspensions that could affect the sorption of neptunium(V) could be various aluminate and silicate species from the partial dissolution of the mineral phase itself. In previous studies on actinide (Cm^{3+}) sorption by the clay minerals kaolinite (Huittinen et al., 2012) and illite (Schnurr et al., 2015), the dissolution of the mineral phase itself in the alkaline pH region (pH > 10) was shown to result in the formation of ternary Cm-silicate complexes on the clay mineral surfaces. Silicon concentrations dissolved from these minerals have been reported to be 1–100 μM from kaolinite (Huittinen et al., 2012) and 40–200 μM from illite (Bradbury and Baeyens, 2009). The Cm-silicate complex was visible on the mineral surface already with silicon concentrations of 10 μM for kaolinite, and 100 μM for illite. The formation of neptunium(V)-silicate complexes have been observed by Pathak and Choppin (2007) and Yusov et al. (2005). Both studies assigned the neptunium(V)-silicate complex to $NpO_2(OSi(OH)_3)$, prevailing in the alkaline pH range. It should be noted that the silicate concentrations were rather high in these studies, 1000–10,000 μM (Pathak and Choppin, 2007) and 4000–20,000 μM (Yusov et al., 2005). The aluminium and silicate concentrations dissolved from our montmorillonite at pH 10 were measured to be 20 and 250 μM (SI Fig. S5), respectively, implying that the silicon concentration in solution would be 250 times as high as the used neptunium(V) concentration in our batch sorption studies. In literature, Myllykylä et al., 2013 and Marty et al., 2011 reported the amount of dissolved silicon from Na-montmorillonite under alkaline conditions to be 300–800 μM, in accordance with our results. Furthermore, the dissolved silicon concentration from montmorillonite was 2.5 to 25 times the amount of silicon sufficient to form a Cm-silicate complex on illite and kaolinite surfaces, respectively. Thus, the dissolution of montmorillonite, and the subsequent formation of soluble neptunium(V)-silicate complexes due to the dissolution of montmorillonite
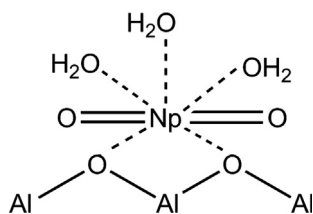
Fig. 6. The proposed neptunyl(V) bidentate surface species on corundum.

as a possible reason for the slight decline in the uptake curve in the alkaline pH range will be investigated in future studies.

To shed some light on the prevailing surface species of neptunium(V) on montmorillonite and corundum, ATR FT-IR experiments were conducted at pH 10 where a sufficient amount of neptunium(V) was sorbed on the mineral surface. Neptunium(V) sorption onto corundum and montmorillonite could be observed in our *in situ* ATR FT-IR experiments from the time-dependent increase of the adsorption band at 790 cm^{-1} (Fig. 4). The sensitivity of this

antisymmetric stretching mode to changes in the coordination environment of the cation has previously been shown on different mineral oxide surfaces (Müller et al., 2009, 2015). For the fully hydrated neptunium(V) cation present in aqueous solution, the v_3 mode is observed at 820 cm^{-1} (Jones and Penneman, 1953) and serves as a reference for the investigation of neptunium(V) complexation reactions (Fig. 4, green line). Coordination of aqueous neptunium (V) ions on surfaces generally reduces the force constants of the O=Np=O bonds. Thus, a displacement of water molecules from the first shell lowers the frequency of the v_3 neptunium(V) stretching mode. The extent of this shift is found to be correlated with the type of surface coordination. Whereas chemical bonding, including deprotonation of the surface groups, results in a considerable red-shift, physical interaction, without deprotonation of the surface groups, reveals only very small shifts because of the remaining intact first hydration sphere (Lefèvre, 2004; Müller et al., 2009). A comparison of the data sets from corundum and montmorillonite (Fig. 4) and from former investigations of TiO$_2$, Al(OH)$_3$ and Fe$_2$O$_3$ (Müller et al., 2009, 2015; Gückel et al., 2013) showed that the frequency
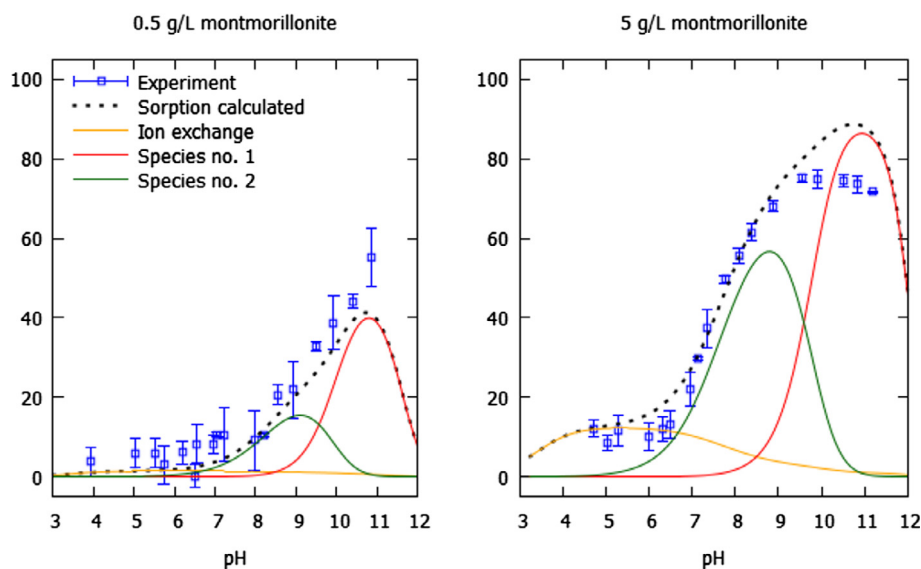

Fig. 7. Modelling of neptunium(V) sorption on 0.5 g/l (left) and 5 g/l (right) montmorillonite in 10 mM NaClO$_4$ solution as a function of pH.

Table 3
Parameters, surface reactions and optimized equilibrium constants used in the surface complexation modelling.

Parameters	Value	Source
Surface site density [mol/g mineral]	6.24×10^{-5}	Tachi et al. (2010)
Specific surface area [m^2/g]	49.8	This study
Reaction	log $K°$	Source
$2{\equiv}XOH + NpO_2^+ + 3H_2O \leftrightarrow ({\equiv}XO)_2NpO_2(H_2O)_3^- + 2\,H^+$	−12.29	This study
$2{\equiv}XOH + NpO_2^+ + 5H_2O \leftrightarrow ({\equiv}XOH)_2NpO_2(H_2O)_5^+$	3.684	This study
${\equiv}X^- + NpO_2^+ \leftrightarrow {\equiv}XNpO_2$	19.42	This study
${\equiv}X^- + Na^+ \leftrightarrow {\equiv}XNa$	20.00	Tachi et al. (2010)
${\equiv}X^- + H^+ \leftrightarrow {\equiv}XH$	21.44	Tachi et al. (2010)
${\equiv}XOH_2^+ \leftrightarrow {\equiv}XOH + H^+$	6.05	Tachi et al. (2010)
${\equiv}XOH \leftrightarrow {\equiv}XO^- + H^+$	−7.79	Tachi et al. (2010)

v_3 of the sorbed neptunium(V) species was observed at $\sim$790 cm^{-1} irrespective of the sorbing surface. The extent of the redshift of $\sim$30 cm^{-1} upon sorption of the neptunium(V) ion on these mineral oxide surfaces suggested a similar type of surface complexation, i.e. the formation of an inner-sphere complex. A slight tailing of the v_3 band (Fig. 4) to higher frequencies may further indicate the presence of other complexes, possibly of outer-sphere character, to a lesser amount. However, the weak sorption capacity of montmorillonite and its strong absorbing background hampered the resolution of coexisting or minor species in IR spectra.

Neptunium(V) uptake by ion exchange observed in the adsorption experiments was also apparent in our desorption study where a montmorillonite suspension, initially equilibrated at pH $\sim$8 to allow for neptunium(V) sorption on the mineral surface, was acidified to pH 5. Here, desorption of neptunium(V) was observed over 250 h and found to reach a plateau at a sorption percentage of approximately 15%, where no further detachment of the actinide from the mineral surface could be detected (Fig. 3, right). In our desorption investigations (Fig. 3) using the replenishment technique, neptunium(V) was almost completely removed from the montmorillonite surface at pH 8, independent of the exchange interval (2–3 days vs. 7 days). At pH 9 and 10 the desorption extent decreased. This could point towards the formation of two different surface complexes on montmorillonite, as necessary in our surface-complexation model, that showed different desorption behaviour from the mineral surface.

In contrast to our batch desorption experiments discussed above, a full detachment of neptunium(V) at pH 10 was observed in our ATR FT-IR studies (Fig. 4, blue traces). The replenishment technique did not fully describe the experimental settings in the IR studies where the mineral surface was constantly flushed with an electrolyte. Thus, neptunium(V) desorption under constant flow conditions should be investigated in more detail in column experiments with adjustable flow parameters. At a first glance, the discrepancy between desorption extents found in literature could be attributed to the very low solid concentration and the relatively high neptunium(V) concentration used in the ATR FT-IR experiments. However, several sorption and desorption studies using the same method have been described in literature, and the desorption kinetics seem to be very different for neptunium(V) sorbed on different mineral phases. In Müller et al. (2009), investigating the sorption of neptunium(V) on TiO$_2$, no inner-sphere complexed neptunium(V) was removed from the mineral surface during the flushing cycle. A similar result was obtained in Gückel et al. (2013), where only a minor amount of neptunium(V) was desorbed from the gibbsite (Al(OH)$_3$) surface upon flushing with the background electrolyte solution. In contrast to these studies and in concordance with the results obtained in the present study, neptunium(V) desorption from hematite (Fe$_2$O$_3$) was significant during the time-frame of the flushing cycle (Müller et al., 2015). To our knowledge an apparent explanation for the different desorption kinetics for neptunium(V) is not available. It is peculiar that two aluminium minerals,

gibbsite and corundum, with reactive aluminol groups on their surfaces showed such large differences in the desorption behaviour of neptunium(V), even though an inner-sphere complex characterized by an absorption band at 790 cm^{-1} was initially present on both mineral surfaces. In Gückel et al. (2013) the inner-sphere sorbed neptunium(V) complex on the gibbsite surface could be assigned to be a bidentate, edge sharing neptunium(V) species based on structural data obtained in EXAFS investigations. In accordance with that study, the very same complex could be used to describe the obtained EXAFS data for neptunium(V) sorption on corundum. This implies that the observed discrepancies in the desorption behaviour cannot be attributed to changes or differences in the neptunium(V) surface complex structures on the two aluminium minerals.

Finally, as the neptunium(V) inner-sphere complexes found in the various ATR FT-IR investigations were characterized by identical sorption bands as found on both corundum and montmorillonite in this study, we tentatively assigned the neptunium(V) inner-sphere complex on montmorillonite to the same bidentate complex found on corundum in our XAS investigations. In order to determine the sorption mechanism of neptunium(V) on montmorillonite, XAS measurements must be performed. Such experiments, however, require highly pure montmorillonite, which is free from impurities (e.g. Zr) interfering with the EXAFS signals at the Np L$_{III}$-edge.

4.2. Surface complexation modelling

In literature, several surface species and combinations thereof can be found to describe the sorption of neptunium(V) on montmorillonite: $\equiv$XO–NpO$_2$ (Bradbury and Baeyens, 2006), $\equiv$XOH–NpO$_2^+$ (Tachi et al., 2010), $\equiv$XO–NpO$_2$(OH)$^-$ (Bradbury and Baeyens, 2006; Tachi et al., 2010), $\equiv$SiOH–NpO$_2^+$ and $\equiv$AlO–NpO$_2$(OH)$^-$ (Turner et al., 1998; Wang et al., 2001). All of these species are monodentate complexes and, thus, do not match our spectroscopic results where a bidentate neptunium(V) complex has been tentatively assigned to form on the montmorillonite surface. The use of different models in the various studies (Turner et al., 1998; Bradbury and Baeyens, 2006; Arai et al., 2007; Gückel et al., 2013) could be correlated with the neptunium(V) surface loading used in the uptake studies (Table 4), where the strong vs. weak site model has been used for low surface loadings (Turner et al., 1998; Bradbury and Baeyens, 2006; Arai et al., 2007) and the DDL model for high surface loadings (Gückel et al., 2013, this study). We tried applying the strong vs. weak site concept using the DDL model, but an unsatisfying fit of the experimental data was obtained. The modelling results showed that three different neptunium complexes were required to explain the neptunium(V) speciation on the montmorillonite surface: ion-exchange with interlayer cations on the permanently charged planar sites in the circumneutral and acidic pH range as well as two pH-dependent surface complexes at pH values above 7 (Fig. 7).

Table 4
The obtained surface loadings in different studies.

Surface area [m²/g]	Solid concentration [g/l]	c (Np(V)) [mol/l]	Surface loading [nmol/m²]	References
97	4.2	9.46×10^{-7}	2.3	Turner et al. (1998)
25	0.6	1×10^{-13}	0.0000067	Bradbury and Baeyens (2006)
25	3.2	1×10^{-13}	0.0000013	Bradbury and Baeyens (2006)
4.5	1.2	3×10^{-6}	560	Gückel et al. (2013)
49.8	0.5	50×10^{-6}	2000	This study
49.8	5	20×10^{-6}	80	This study

The ion exchange reaction on montmorillonite sorption experiments could be modelled with an equilibrium constant ($\log K$) of 19.42 (Tachi et al., 2010).

Our spectroscopic investigations did not indicate the formation of any other surface complexes except the one bidentate edge-sharing inner-sphere complex. However, a slight tailing of the adsorption band for montmorillonite was observed in the ATR FT-IR studies that could indicate the presence of a second complex, possibly of outer-sphere character. Our modelling showed that three neptunium(V) species are formed on the montmorillonite surface: ion exchanged neptunium(V) and two pH-dependent surface complexes (species 1 and species 2). Species 1 corresponds to the spectroscopically identified bidentate inner-sphere complex associated with the release of protons from the surface hydroxyl groups. Species 2 on the other hand does not cause deprotonation of surface hydroxyls, however, the exact character, whether outer-sphere or inner-sphere bound to the montmorillonite surface can not be resolved using the DDL model. Previously the formation of neptunium(V) surface complexes (even though with different denticity as in our study) on montmorillonite has been modelled by Turner et al. (1998), Wang et al., (2001), and Tachi et al. (2010). Both Turner et al. (1998) and Wang et al. (2001) modelled the surface complex associated with no proton release from the surface on the silanol groups ($\equiv$SiOH–NpO$_2^+$) and the surface complex accompanied by proton release on the aluminol groups ($\equiv$AlO–NpO$_2$ (OH)$^-$), while Tachi et al. (2010) used generic surface groups for the neptunium(V) complexes, i.e. $\equiv$SOH–NpO$_2^+$ and $\equiv$SO–NpO$_2$(OH)$^-$. The equilibrium constants, despite the different denticities of the surface complexes used in the above mentioned studies and in our study, are comparable with 2.85 (Tachi et al., 2010), 3.04 (Wang et al., 2001), 4.05 (Turner et al., 1998), and 3.68 (this study) for the pH-dependent complex without the release of surface protons (species 2) and -14.0, -13.72, $-13,79$, and $-12,29$, respectively for the inner-sphere complex accompanied by proton release (species 1).

The modelled inner-sphere complex was slightly overestimated in comparison to the experimental batch sorption data for the 5 g/l montmorillonite concentration (Fig. 7). Our model predicted a decline of the neptunium(V) uptake above pH 11 due to the predominance of negatively charged NpO$_2$(OH)$_2^-$ complexes in solution. Up to this pH, however, 90% of the added neptunium(V) should be attached to the surface. In our batch study the maximum uptake of neptunium(V) is just below 80% followed by a decrease of the uptake above pH 10. As previously discussed, this sorption behaviour could be caused by the formation of neptunium(V)-silicate complexes.

5. CONCLUSIONS

In this study we investigated the uptake and speciation of neptunium(V) on montmorillonite and corundum under carbonate-free conditions. A complete removal (close to 100% sorption) of the neptunium(V) cation from the aqueous phase, however, was not obtained in any of the batch sorption experiments with mineral concentrations of 0.5 g/l and 5 g/l. Our batch desorption studies indicated a strong pH-dependent removal of neptunium(V) from both the corundum and montmorillonite surfaces. This desorption behaviour suggested that different surface complexes with differing desorption kinetics were forming on the mineral surfaces. Neptunium(V) removal from the corundum and montmorillonite surfaces could also be observed in our ATR-FT IR investigations, where a complete removal on the neptunium(V) sorption complex characterized by an absorption band at 790 cm^{-1} was observed. This highly removable neptunium(V) complex was assigned, analogous to previous studies, to a bidentate, edge-sharing inner-sphere complex on the corundum and montmorillonite surfaces. This assignment was supported by the structural parameters obtained in our EXAFS studies for neptunium(V) sorption on corundum. Finally, surface complexation modelling of neptunium(V) sorption on montmorillonite suggested the formation of two pH-dependent surface complexes on the mineral surface above pH 7. Below pH 7, the uptake of neptunium(V) on montmorillonite occurred via cation exchange on negatively charged planar sites. The pH-dependent surface complex (species 1) associated with the deprotonation of surface groups could be assigned to a bidentate edge sharing inner-sphere complex based on our spectroscopic data. Whether the pH-dependent complex in the circumneutral to slightly alkaline pH-range (species 2) is of outer-sphere character or alternatively bound to different surface groups than species 1 (e.g. silanol vs. aluminol), however, cannot be deduced from the surface complexation model.

APPENDIX A. SUPPLEMENTARY DATA

Supplementary data associated with this article can be found, in the online version, at http://dx.doi.org/10.1016/j.gca.2016.10.040.

REFERENCES

Allen P. G., Bucher J. J., Shuh D. K., Edelstein N. M. and Reich T. (1997) Investigation of aquo and chloro complexes of UO_2^{2+}, NpO_2^+, Np^{4+}, and Pu^{3+} by X-ray absorption fine structure spectroscopy. *Inorg. Chem.* **36**, 4676–4683.

Ankudinov A. L., Ravel B., Rehr J. and Conradson S. D. (1998) Real-space multiple-scattering calculation and interpretation of X-ray-absorption near-edge structure. *Phys. Rev. B* **58**, 7565–7576.

Appelo C. A. J. and Parkhurst D. L. (2013). Calculating cation exchange with PHREEQC (Version 2), *http://www.hydrochemistry.eu/pub/ap_pa02.pdf*.

Arai Y., Moran P. B., Honeyman B. D. and Davis J. A. (2007) In situ spectroscopic evidence for neptunium(V)-carbonate inner-sphere and outer-sphere ternary surface complexes on hematite surfaces. *Environ. Sci. Technol.* **41**, 3940–3944.

Benedicto A., Begg J. D., Zhao P., Kersting A. B., Missana T. and Zavarin M. (2014) Effect of major cation water composition on the ion exchange of Np(V) on montmorillonite: $NpO_2^+–Na^+–K^+–Ca^{2+}–Mg^{2+}$ selectivity coefficients. *Appl. Geochem.* **47**, 177–185.

Birgersson M. and Karnland O. (2009) Ion equilibrium between montmorillonite interlayer space and an external solution–consequences for diffusional transport. *Geochim. Cosmochim. Acta* **73**, 1908–1923.

Bradbury M. H. and Baeyens B. (1997) A mechanistic description of Ni and Zn sorption on Na-montmorillonite Part II: Modelling. *J. Contam. Hydrol.* **27**, 223–248.

Bradbury M. H. and Baeyens B. (2002) Sorption of Eu on Na- and Ca-montmorillonites: experimental investigations and modelling with cation exchange and surface complexation. *Geochim. Cosmochim. Acta* **66**, 2325–2334.

Bradbury M. H. and Baeyens B. (2006) Modelling sorption data for the actinides Am(III), Np(V) and Pa(V) on montmorillonite. *Radiochim. Acta* **94**, 619–625.

Bradbury M. H. and Baeyens B. (2009) Sorption modelling on illite; Part I, titration measurements and the sorption of Ni, Co, Eu and Sn. *Geochim. Cosmochim. Acta* **73**, 990–1003.

Del Nero M., Assada A., Madé B., Barillon R. and Duplâtre G. (2004) Surface charges and Np(V) sorption on amorphous Al and Fe silicates. *Chem. Geol.* **211**, 15–45.

Guillaumont R., Fanghänel T., Fuger J., Grenthe I., Neck V., Palmer D. A. and Rand M. H. (2003) *Update on the Chemical Thermodynamics of Uranium, Neptunium, Plutonium, Americium and Technetium*. Elsevier, Amsterdam.

Gückel K., Rossberg A., Müller K., Brendler V., Bernhard G. and Foerstendorf H. (2013) Spectroscopic identification of binary and ternary surface complexes of Np(V) on gibbsite. *Environ. Sci. Technol.* **47**, 14418–14425.

Hartmann E., Brendebach B., Polly R., Geckeis H. and Stumpf T. (2011) Characterization and quantification of Sm(III)/ and Cm (III)/clay mineral outer-sphere species by TRLFS in D_2O and EXAFS studies. *J. Colloid Interface Sci.* **353**, 562–568.

Huittinen N., Rabung T., Lützenkirchen J., Mitchell S. C., Bickmore B. R., Lehto J. and Geckeis H. (2009) Sorption of Cm(III) and Gd(III) onto gibbsite, α-Al(OH)$_3$: a batch and TRLFS study. *J. Colloid Interface Sci.* **332**, 158–164.

Huittinen N., Rabung T., Schnurr A., Hakanen M., Lehto J. and Geckeis H. (2012) New insight into Cm(III) interaction with kaolinite – influence of mineral dissolution. *Geochim. Cosmochim. Acta* **99**, 100–109.

Hursthouse A. S., Baxter M. S., Livens F. R. and Duncan H. J. (1991) Transfer of sellafield-derived Np-237 to and within the terrestrial environment. *J. Environ. Radioact.* **14**, 147–174.

Ikeda-Ohno A., Hennig C., Rossberg A., Funke H., Scheinost A. C., Bernhard G. and Yaita T. (2008) Electrochemical and complexation behavior of neptunium in aqueous perchlorate and nitrate solutions. *Inorg. Chem.* **47**, 8294–8305.

Jones L. H. and Penneman R. A. (1953) Infrared spectra and structure of uranyl and transuranium (V) and (VI) ions in aqueous perchloric acid solution. *J. Chem. Phys.* **21**, 542–544.

Kaszuba J. P. and Runde W. H. (1999) The aqueous geochemistry of neptunium: dynamic control of soluble concentrations with applications to nuclear waste disposal. *Environ. Sci. Technol.* **33**, 4427–4433.

Koningsberger D. C. and Prins R. (1988) *X-ray absorption: Principles, Applications, Techniques of EXAFS, SEXAFS, and XANES*. John Wiley and Sons, New York, NY.

Kozai N., Yamasaki S. and Ohnuki T. (2014) Application of simplified desorption method to study on sorption of neptunium(V) on montmorillonite-based mixtures. *J. Radioanal. Nucl. Chem.* **299**, 1581–1587.

Kumpulainen S. and Kiviranta L. (2010) Mineralogical and chemical characterization of various bentonite and smectite-rich clay materials. *Working Rep.*, 2010–52.

Kupcik T., Rabung T., Lützenkirchen J., Finck N., Geckeis H. and Fanghänel T. (2016) Macroscopic and spectroscopic investigations on Eu(III) and Cm(III) sorption onto bayerite (β-Al (OH)$_3$) and corundum (α-Al$_2$O$_3$). *J. Colloid Interface Sci.* **461**, 215–224.

Lefèvre G. (2004) In situ Fourier-transform infrared spectroscopy studies of inorganic ions adsorption on metal oxides and hydroxides. *Adv. Colloid Interface Sci.* **107**, 109–123.

Lemire R. J., Fuger J., Spahiu K., Nitsche H., Sullivan J. C., Ullman W. J., Potter P., Vitorge P., Rand M. H., Wanner H. and Rydberg J. (2001) *Chemical Thermodynamics of Neptunium and Plutonium*. Elsevier, Amsterdam.

Marques Fernandes M., Baeyens B., Dähn R., Scheinost A. C. and Bradbury M. H. (2012) U(VI) sorption on montmorillonite in the absence and presence of carbonate: a macroscopic and microscopic study. *Geochim. Cosmochim. Acta* **93**, 262–277.

Marty N. C. M., Cama J., Sato T., Chino D., Villiéras F., Razafitianamaharavo A., Brendlé J., Giffaut E., Soler J. M., Gaucher E. C. and Tournassat C. (2011) Dissolution kinetics of synthetic Na-smectite. An integrated experimental approach. *Geochim. Cosmochim. Acta* **75**, 5849–5864.

Matz W., Schnell N., Bernhard G., Prokert F., Reich T., Claussner J., Oehme W., Schlenk R., Dienel S., Funke H., Eichhorn F., Betzl M., Pröhl D., Strauch U., Hüttig G., Krug H., Neumann W., Brendler V., Reichel P., Denecke M. A. and Nitsche H. (1999) ROBL – a CRG beamline for radiochemistry and materials research at the ESRF. *J. Synchrotron Radiat.* **6**, 1076–1085.

Missana T., Benedicto A., Garcia-Gutierrez M. and Alonso U. (2014) Modeling cesium retention onto Na-, K- and Ca-smectite: effects of ionic strength, exchange and competing cations on the determination of selectivity coefficients. *Geochim. Cosmochim. Acta* **128**, 266–277.

Müller K., Foerstendorf H., Brendler V. and Bernhard G. (2009) Sorption of Np(V) onto TiO_2, SiO_2, and ZnO: an in situ ATR FT-IR spectroscopic study. *Environ. Sci. Technol.* **43**, 7665–7670.

Müller K., Foerstendorf H., Meusel T., Brendler V., Lefevre G., Comarmond M. J. and Payne T. E. (2012) Sorption of U(VI) at the TiO_2-water interface: An in situ vibrational spectroscopic study. *Geochim. Cosmochim. Acta* **76**, 191–205.

Müller K., Gröschel A., Rossberg A., Bok F., Franzen C., Brendler V. and Foerstendorf H. (2015) In situ spectroscopic identification of neptunium(V) inner-sphere complexes on the hematite-water interface. *Environ. Sci. Technol.* **49**, 2560–2567.

Myllykylä E., Tanhua-Tyrkkö M., Bouchet A. and Tiljander M. (2013) Dissolution experiments of Na- and Ca-montmorillonite in groundwater simulants under anaerobic conditions. *Clay Miner.* **48**, 295–308.

Nagasaki S. and Tanaka S. (2000) Sorption equilibrium and kinetics of NpO_2^+ on dispersed particles of Na-montmorillonite. *Radiochim. Acta* **88**, 705–709.

Parkhurst D. L. and Appelo C. A. J. (2013) Description of input and examples for PHREEQC version 3; a computer program for speciation, batch-reaction, one-dimensional transport, and inverse geochemical calculations. *U. S. Geological Survey Techniques and Methods* **06-A43**.

Pathak P. N. and Choppin G. R. (2007) Silicate complexation of NpO_2^+ ion in perchlorate media. *J. Radioanal. Nucl. Chem.* **274**, 3–7.

Poeter E. P., Hill M. C., Banta E. R., Mehl S. and Christensen S. (2006) UCODE_2005 and six other computer codes for universal sensitivity analysis, calibration, and uncertainty evaluation constructed using the JUPITER API. *U. S. Geological Survey Techniques and Methods* **06-A11**.

Ressler T. (1998) WinXAS: a program for X-ray absorption spectroscopy data analysis under MS-Windows. *J. Synchrotron Radiat.* **5**, 118–122.

Sabodina M. N., Kalmykov S. N., Sapozhnikov Yu. A. and Zakharova E. V. (2006) Neptunium, plutonium and ^{137}Cs sorption by bentonite clays and their speciation in pore waters. *J. Radioanal. Nucl. Chem.* **270**, 349–355.

Schnurr A., Marsac R., Rabung T., Lützenkirchen J. and Geckeis H. (2015) Sorption of Cm(III) and Eu(III) onto clay minerals under saline conditions: batch adsorption, laser-fluorescence spectroscopy and modeling. *Geochim. Cosmochim. Acta* **151**, 192–202.

Soderholm L., Antonio M. R., Williams C. and Wasserman S. R. (1999) XANES spectroelectrochemistry: a new method for determining formal potentials. *Anal. Chem.* **71**, 4622–4628.

Soltermann D., Baeyens B., Bradbury M. H. and Marques Fernandes M. (2014) Fe(II) uptake on natural montmorillonites. II. Surface complexation modeling. *Environ. Sci. Technol.* **48**, 8698–8705.

Stumpf T., Bauer A., Coppin F. and Kim J. I. (2001) Time-resolved laser fluorescence spectroscopy study of the sorption of Cm(III) onto smectite and kaolinite. *Environ. Sci. Technol.* **35**, 3691–3694.

Tachi Y., Nakazawa T., Ochs M., Yotsuji K., Suyama T., Seida Y., Yamada N. and Yui M. (2010) Diffusion and sorption of neptunium(V) in compacted montmorillonite: effects of carbonate and salinity. *Radiochim. Acta* **98**, 711–718.

Tombácz E. and Szekeres M. (2004) Colloidal behavior of aqueous montmorillonite suspensions: the specific role of pH in the presence of indifferent electrolytes. *Appl. Clay Sci.* **27**, 75–94.

Turner D. R., Pabalan R. T. and Bertetti F. P. (1998) Neptunium (V) sorption on montmorillonite: an experimental and surface complexation modeling study. *Clays Clay Miner.* **46**, 256–269.

Turner G. D., Zachara J. M., McKinley J. P. and Smith S. C. (1996) Surface-charge properties and UO_2^{2+} adsorption of a subsurface smectite. *Geochim. Cosmochim. Acta* **60**, 3399–3414.

Virtanen S., Bok F., Ikeda-Ohno A., Rossberg A., Lützenkirchen J., Rabung T., Lehto J. and Huittinen N. (2016) The specific sorption of Np(V) on the corundum (α-Al_2O_3) surface in the presence of trivalent lanthanides Eu(III) and Gd(III): a batch sorption and XAS study. *J. Colloid Interface Sci.* **483**, 334–342.

Viswanathan H. S., Robinson B. A., Valocchi A. J. and Triay I. R. (1998) A reactive transport model of neptunium migration from the potential repository at Yucca Mountain. *J. Hydrol.* **209**, 251–280.

Wang P., Anderko A. and Turner D. R. (2001) Thermodynamic modeling of the adsorption of radionuclides on selected minerals. I: Cations. *Ind. Eng. Chem. Res.* **40**, 4428–4443.

Yusov A. B., Fedoseev A. M., Isakova O. V. and Delegard C. H. (2005) Complexation of Np(V) with silicate ions. *Radiochemistry* **47**, 39–43.

Zavarin M., Powell B. A., Bourbin M., Zhao P. and Kersting A. B. (2012) Np(V) and Pu(V) ion exchange and surface-mediated reduction mechanisms on montmorillonite. *Environ. Sci. Technol.* **46**, 2692–2698.

Zhao P., Tinnacher R. M., Zavarin M. and Kersting A. B. (2014) Analysis of trace neptunium in the vicinity of underground nuclear tests at the Nevada National Security Site. *J. Environ. Radioact.* **137**, 163–172.

Associate editor: Christophe Tournassat